San LuisTolentino
M.Sc. Mech. Ing.
National Experimental Polytechnic University"AJS" Vice-Rectorate (UNEXPO), Puerto Ordaz. Bolívar
Venezuela
Research collaborator
Group of Mathematical Modeling and Numerical Simulation (GMMNS)
National University of Engineering (UNI)
Lima
Perú

Jorge Mirez
Dr.& MSc Physics, Mech. Electrical Eng.
Group of Mathematical Modeling and Numerical Simulation (GMMNS)
Faculty of Petroleum, Natural Gas and Petrochemical Engineering
National University of Engineering (UNI)
Lima
Perú

Throat Length Effect on the Flow Patterns in Off-Design Conical Nozzles

In the present work, a flow field study was performed for off-design conical nozzles with non-circular cylindrical throat sections such as those found in experimental sounding rocket motor applications. The flow field was simulated with the RANS model in ANSYS-Fluent R16.2 code for 2D domains. The governing equations used are conservation of mass, momentum, energy, and state. Sutherland's equation for viscosity as a function of temperature and the Spalart-Allmaras turbulence model was used to simulate overexpanded flow turbulence. The results showed pressure and Mach number fluctuations as the throat length increased. In the throat section, it is concluded that for the length range of 5 to 15% of the throat diameter, the flow accelerates without the presence of internal shock.

Keywords: *flow field, internal shock, fluctuation, throat length, Mach number, pressure, off-design conical nozzles.*

1. INTRODUCTION

In the aerospace field, supersonic nozzles are used in rocket engines to generate thrust. Its dimensions are variable, which depend on the power required to create the rocket's thrust carrying the payload.

In the academic field, some universities have focused on the development of sounding rockets based on academic projects for research purposes, which include the design of the nozzle, structure, fuel, and measuring instruments for atmospheric data collection, among other studies [1-7]. The Amelia small rocket program exposes the scope of their research for altitudes of 10 km, and as the propellant, they use solid fuel [1]. The sounding rocket program in Peru was developed with the main objective of delivering a small scientific payload of 5 to 80 kg for suborbital flights from 80 to 200 km maximum altitude [3], as well as the development of sounding rockets by the Group of Atmospheric and Space Sciences (GCEA), where the experimental nozzles have a throat length [6].

The flow in supersonic nozzles is studied repeatedly to optimize the new geometries of the walls to achieve better development of the flow regime.

Nozzle designs are based on the mean angle, α, of the diverging section, which is 12° to 18° [8]. Nozzles with mean angles $\alpha < 12°$ are classified as off-design nozzles.

The behavior of the flow inside the nozzle depends on the inlet pressure and the ambient pressure of the atmosphere. The difference between these two pressures determines whether the flow is overexpanded, adapted, orunderexpanded [8], [9].

For overexpanded flow conditions, adverse pressure gradients, flow separation, and recirculation, detachment of the boundary layer from the wall occurs [10-12]. The turbulent boundary layer [12] interacts with the shock wave and causes instability in its position, where the shock wave is composed of the oblique shock, which is the weak shock, and the normal shock, which is the stronger one. The transition of free shock, vortices [13], asymmetry of lateral pressure loads on the wall [12], and influence on the Mach disk at the nozzle outlet by radial pressure gradients [14] are also presented. As well as, the Prandtl-Meyer expansion waves [10] appear at the edges of the nozzle exit; therefore, velocity, pressure, temperature, and density fluctuate in different regions of the flow field [10-12].

The use of instruments for recording temperatures in the flow field by experimental means allows for determining the magnitudes in the walls and different regions of the flow [15]. The thermal effect on an experimental conical nozzle wall is illustrated in Fig. 1 [16], which shows a characteristic color tone for steel materials when they reach high temperatures. The wall region forms a ring with a darker color tone between high and low temperatures, different from other regions. In that region, a thermal shock occurs. The temperature gradient distributed along the nozzle wall interacts with the internal and external flow. Therefore, in the inner wall of the divergent, the temperature increases as a result of the friction of a region of the flow that moves at high-speed brushing against the wall. The flow region adjacent to the wall corresponds to the thermal boundary layer [12]. In the central region, the temperature of the supersonic jet decreases as the flow expands.

In the experimental tests, the Schlieren technique [17] allows capturing the shapes of the shock waves. However, this technique does not allow the thermodynamic parameters of the flow to be quantified. Meanwhile, computational fluid dynamics (CFD) [18] allows the reproduction of the shapes of shock waves and quantifies the magnitudes of thermodynamic parameters, such as pressure, temperature, and speed. Different turbulence models [19] used in CFD are reported

Received: December 2021, Accepted: March 2022
Correspondence to: San LuisTolentino, Group of Mathematical Modeling and Numerical Simulation, National University of Engineering (UNI), Lima, Perú
E-mail: sanluist@gmail.com
doi:10.5937/fme2201271T

in the literature. In addition, the flow at the nozzle exits for complex geometries that employ flow control mechanisms can be studied through experimental tests and computational simulations [20-22].

Figure 1. The conical nozzle was subjected to experimental static testing by Riveros and Rodriguez [16].

Conventional nozzles have a curvature in the throat section. The sonic line is a curve that develops the flow, as presented by Cuffel et al. [23], the Mach number distribution in the transonic region. Sauer's method [24] is based on the theory of small perturbations, which allows the design of radii of curvatures. For small radii of curvature, we have the proposal of Kliegel and Levin [25], Back and duffel [26], and Haddad and Kbab [27], with which sonic lines can be used to start the cal–culations of the supersonic flow field using the method of characteristics (MoC). It should be noted that the Mach number gradients are different between models of quasi-one-dimensional isentropic flow and viscous flow, and this is because the viscous flow in CFD takes into account the velocity boundary layer and the boundary layer thermal [12].

The design of a group of experimental nozzles with throat length, L_g, used in sounding rocket motors for research purposes [6], [28] achieved their design ob–jectives in static and dynamic tests. The length of the throat, L_g, of the experimental nozzles tested in soun–ding rockets [6], [28] has an approximate dimension to their diameter, D_g. It should be noted, in the throat section, the geometry of these types of nozzles is different from conventional nozzles that are designed with a curvature in the throat section. Consequently, the development of the flow in the throat section is different with respect to the flow regime that develops in a conventional nozzle.

Numerical studies of the simulation of the turbu–lence of the overexpanded flow applying CFD for a group of nozzles with throat length reported internal shocks in the throat section, where the flow presented fluctuations in Mach number velocity and pressure gradients [29-32].

The presence of internal shocks in the throat section is a consequence of a throat length that is too long. Therefore, establishing an optimal length of the throat section would avoid internal shocks in said section. In addition, approaching the study for nozzles with throat lengths that are longer than those reported in [29], [30], [31], [32] would allow obtaining results on the behavior of speed and intensity fluctuations propagation of internal shocks. And this contributes to expanding the physical knowledge of flow development for a wider range in the throat section.

The present work aims to analyze the Mach number and pressure-flow field for 2D computational domains of conical nozzles with throat length, with a mean divergent angle $\alpha = 10°$. The study is carried out for different throat lengths, L_g, up to a limit equivalent to twice its diameter, to determine an optimal range of the throat length so that there are no speed fluctuations. Flow field turbulence is simulated with ANSYS-Fluent R16.2 code. Section 2 presents the methodology. In section 3, the results of pressure and Mach number are presented. Next, section 4 presents the conclusions.

2. METHODOLOGY

2.1 Governing equations and flow conditions

The overexpanded flow field for an off-design conical nozzle was simulated at a steady state in ANSYS Fluent R16.2 code. The Reynolds-averaged Navier-Stokes equations (RANS) were used. The governing equations are the equation of conservation of mass, momentum, energy, and the ideal gas equation [33].

The flow at the nozzle inlet was considered as an ideal gas with a specific heat ratio $k = 1.4$, gas constant $R = 287$ J/(kg·K), specific heat at constant pressure $C_p = 1006.43$ J/(kg·K), and thermal conductivity $k = 0.042$ W/(m·K) [33]. This consideration for an ideal gas is adequate since it allows the flow to be homogeneous at the nozzle inlet.

The dominant parameter for compressible flow is the Mach number M. The considerations are as follows: for incompressible flow $M < 0.3$; subsonic flow $0.3 < M < 0.8$; transonic flow $0.8 < M < 1.2$; supersonic flow $1.2 < M < 5$; hypersonic flow $M > 5$; sonic flow $M = 1$ [34]. Regarding hypersonic flow, White [34] considers Mach 3 and Anderson [9] from Mach 5.

2.2 Computational domain and meshing

The flow analysis was considered to design a conical nozzle with area ratio $A/A^* = 5.811$ and Mach number 3.33. Due to the symmetry of the conical nozzle, it was considered to simulate the flow for 2D domains with axial symmetry on the x-axis. The computational domain and the meshing are shown in Fig. 2.

The basic dimensions of the conical nozzle are as follows: converging section $L_c/D_g = 1.5$, diverging section $L_c/D_g = 4$. Throat diameter $D_g = 20$ mm. Throat length L_g is variable in the range of $0.05 \leq L_g/D_g \leq 2$. The mean angle of the convergent $\beta = 30°$ and the divergent $\alpha = 10°$. The throat section has no curvature at its ends that joins the converging and diverging sec–tions. At the outlet of the nozzle, the wall has a thic–kness of 5 mm.

A short section of the combustion chamber of length $0.25D_g$ was included in the domain to direct the flow. Also, a section for the discharge of the flow into the atmosphere was included, being the length of the domain of the atmosphere in the horizontal direction $8D_g$ and the vertical direction $1.955D_g$.

The section of the domain in the region of the flow in the atmosphere that was taken into consideration is in accordance with the student's interest since the effect of gravity is not included. The flow field is symmetric around the axis of the nozzle. This considerably reduces the number of mesh elements and data processing time during iterations. In the flow studies where the effect of gravity is included, larger domains should be included according to the flow discharge distance since the flow leaving the nozzle has a high speed with gradients of pressure, temperature, and shock waves. Upon contact with the flow region of the atmosphere, mixing occurs in different directions. Due to the difference in density, the regions of hot gases rise, and the regions of cold gases descend due to the convective phenomenon.

In total, 13 domains were considered for the study of the flow field, from which the nine domains for throat length in the range of L_g/D_g = 0.05 – 0.45, with an inc–rement of 0.05; and four domains for the range of L_g/D_g = 0.5 - 2, with an increment of 0.5. It should be noted that Fig. 2 is only shown in the domain with L_g/D_g = 0.05.

The boundary conditions for the thirteen domains we re set asstagnation pressure and temperature at the inlet of the nozzle P_0 = 1200 kPaand T_0 = 1620 K. The ambient pressure and temperature of the atmosphere P = 100 kPa and T = 300 K. The nozzle pressure ratio was NPR = 12.

Due to the symmetry of the conical nozzles, it was considered to simulate 2D domains with axial symmetry on the x-axis. This considerably reduces the number of mesh elements and data processing time during itera–tions.

The domain walls were considered adiabatic. The flow velocity in the walls is null due to the no-slip condition. In axial symmetry, the flow velocity is zero in the radial direction. As well as, the domains were meshed with quadrilateral cells and refined in the walls by the presence of shear stresses, as shown in the details of Fig. 2.

The numerical convergence study was performed for three meshes, and flow simulation for *NPR=12*. The domains were meshed in the ANSYS-Meshing platform and discretized using ICEM-CFD interaction. A high mesh density was applied, being the first mesh with 30813 elements, the second with 31110 elements, and the third with 32121 elements. It should be noted that the meshing in the nozzle section was divided in the radial direction with 100 elements and in its length with 155 elements, with the size of the cell in the radial direction being 0.1 mm. For each refinement in the wall region, 16565 elements were obtained for the first mesh, 16864 for the second, and 17105 elements in the third, being the size of the refined cells adjacent to the wall of 0.033 mm.

For the meshed domain of Fig. 2, ANSYS-Fluent R16.2 reported: Mesh quality: minimum orthogonal quality 0.221096; orthogonal quality ranges from 0 to 1, where values close to 0 correspond to low quality. Maximum ortho skew 0.778288; ortho skew ranges from 0 to 1, where values close to 1 correspond to low quality. Maximum aspect ratio 40.6345. For inflation: transition ratio 0,272; maximum layers 2; and growth rate 1.2.

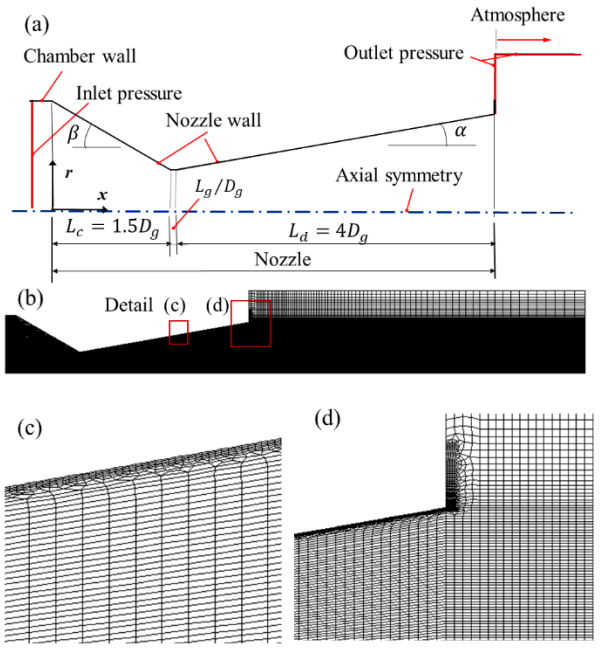

Figure 2. Conical nozzle geometry. (a) Computational domain and boundary conditions. (b) Meshed domain with 30813 elements. The enlarged detail (c) and (d) show the refined mesh in the wall region. Source: Authors.

In the flow region adjacent to the nozzle wall, ANSYS-Fluent R16.2 reported variations of y^+ in the range from 1 to 23. The highest values are presented at the entrance of the throat, at position x/D_g = 1.5, and at the nozzle outlet, as shown in Fig. 3.

For the three meshed domains, simulations for NPR = 12 yielded similar results for Mach number 3.35 at the nozzle exit. With the analytical equation of Stodola (8) [9], [34], which is applied to nozzle design, Mach number 3.33 was obtained. When comparing both Mach number values, the absolute error of 0.02 was obtained.

The mass flow for the three meshed domains was 0.355 kg/s, with errors around 4.7×10^{-6}. While, with the analytical equation for quasi-one-dimensional isentropic flow, the mass flow of 0.378 kg/s was obtained. It was the absolute error in the numerical solution of 0.023.

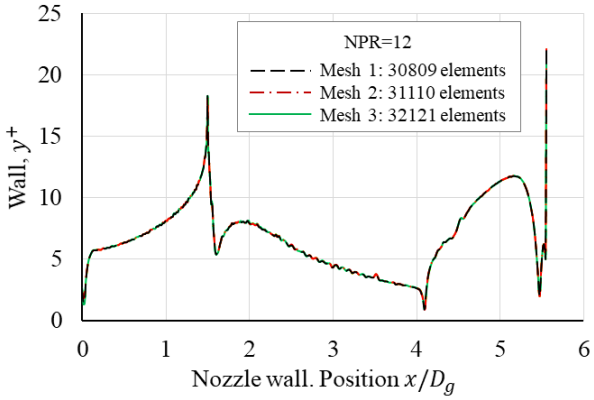

Figure 3. The behavior of y^+ in the nozzle wall for three meshed domains. Source: Authors.

2.3 Computational solution method

In the ANSYS-Fluent R16.2 code, the solution option for density-based analysis for a compressible fluid and 2D axial symmetry was considered. The Spalart-

Allmaras S-A model [35] was chosen for flow turbulence, and Sutherland's law [36] was used for flow viscosity as a function of temperature. The implicit formulation and Roe-FDS flow type were considered for the solution method. For spatial discretization, the gradient: Least Squares Cell-Based. For flow, kinetic energy turbulence, and specific dissipation, the option: Second-Order Upwind was selected. For the residual monitor, a fixed value of $1x10^{-6}$was determined, both for continuity, speed, and energy. The hybrid initi–alization method was applied. 26000-87000 iterations were performed to obtain the Mach number and pres–sure-flow field results.

A computer with the following characteristics was used for data processing: Dell brand CPU, Optiplex 7010 model, i5 3470, four 3.2 GHz processors, and 8 GB RAM.

2.4 Validation of the turbulence model S-A

The Spalart-Allmaras S-A turbulence model [35] is composed of a single equation and satisfies the respon–ses to adverse pressure gradients and boundary layer separation. Its application in the turbulence simulations of the present work was validated with experimental pressure data reported in the work of Hunter [37].

The S-A turbulence model [35] was compared with Menter's SSTk - ω model [38] for an overexpanded flow in a 2D computational domain for a flat nozzle [37]. The pressure profiles on the nozzle wall of the S-A and SSTk - ω turbulence models are shown in Fig. 4, where the curve for the SA model has a better fit in the region where the smallest pressure drop occurs. Pressure when compared with experimental data [37].

In the computational simulation, the S-A and SSTk - ω models were used without modifying their structure and constants. It should be noted that the same metho–dology reported in [39] was applied for the simulation of the flow.

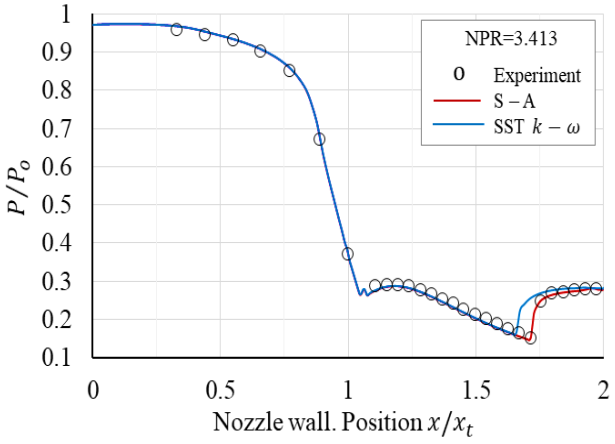

Figure 4. Wall Pressure for NPR=3.413.Source: Hunter experiment [37]. Source: Simulation, Authors.

3. RESULTS AND DISCUSSION

The Mach number and pressure-flow field simulations (Fig. 5 and 7) show the internal shocks in the throat section and oblique shocks in the divergent section and the normal shock wavefront. (Mach disk) that occurs outside the nozzle. The region where the flow and boundary layer separation begin is observed, and the region where recirculation occurs after flow separation is adjacent to the nozzle wall (Fig. 7). In addition, the results show the behavior of the pressure and Mach number patterns in the nozzle section (Fig. 6 and 8).

The throat section starts at position x/D_g = 1.5, and from this position, the throat length increases in the range of $0.05 \leq L_g/D_g \leq 2$, for the final position x/D_g – 3.5. And this range is study interest to know what effect the increase in throat length has on the behavior of the flow in said section and the divergent section. The pressure and Mach number patterns and the develop–ment of internal shocks in the throat section in the range from position x/D_g = 1.5 to x/D_g = 3.5 are shown in Fig. 5, 6, 7, and 8.

In the throat section for x/D_g = 0.05, which is located from position x/D_g = 1.5 to x/D_g = 1.55, and L_g/D_g = 0.15, which is located from position x/D_g = 1.5, up to x/D_g = 1.65, the flow development, transition in said section is very slight. However, it affects the flow region in the divergent as shown in Fig. 5a, 5b, 6a, 7a, 7b, 8a. For x/D_g = 0.2, the Mach number pattern presents two peaks below Mach 1.9 and 2.5, while for x/D_g = 0.05 it presents a single peak at position x/D_g = 2.8, for a value below Mach 3 (Fig. 8a). In both cases, the peaks are still outside the throat section since for L_g/D_g = 0.2 the throat section ends at position x/D_g = 1.7.

The flow in the throat section accelerates. In the divergent section, it fluctuates, while at the nozzle exit, for the range of $0.05 \leq L_g/D_g \leq 0.15$, the flow has a speed around Mach 3.35, and for L_g/D_g = 0.2 the speed decreases to Mach 3.13 (Fig. 8a). Therefore, the performance decreases slightly when there is a slight drop in speed at the nozzle outlet.

The transition of the flow development in the throat section is more accentuated from L_g/D_g = 0.25. As L_g increases, the internal shocks, which are oblique waves, are formed towards the regions adjacent to the walls of the throat section (Fig. 5c, 5d, 5e, and 7c, 7d, 7e). For the range of $0.25 \leq L_g/D_g \leq 0.45$, the behavior of the fluctuations has similar patterns in the divergent, and near the throat, there is a normal shock wave of Mach 1.71. In the throat section, the flow is accelerated up to Mach 1.57. For L_g/D_g = 0.45, the final length of the groove is located at position x/D_g = 1.95 (Fig. 6c and 8b). When the nozzle has L_g/D_g = 0.5, the flow is still accelerating until the end of the throat section, while oblique impingement is present at the ends. The normal shock occurs as the flow exits the throat and accelerates back toward the outlet.

For L_g/D_g = 1, the throat length, L_g, is equivalent to its diameter, D_g, and the throat section is located in the range from position x/D_g = 1.5 to x/D_g = 2.5. The Mach number reaches a maximum and minimum value in the range of 0.6 < M < 1.8 (Fig. 8c), and the oblique shocks are well defined (Fig. 5g and 7g).

As the length of the throat increases for L_g/D_g = 1.5 and L_g/D_g = 2, the internal shocks increase with less intensity (Fig. 5h, 5i, 7h, 7i), and the flow fluctuations decrease in transonic speed (Fig. 8c).

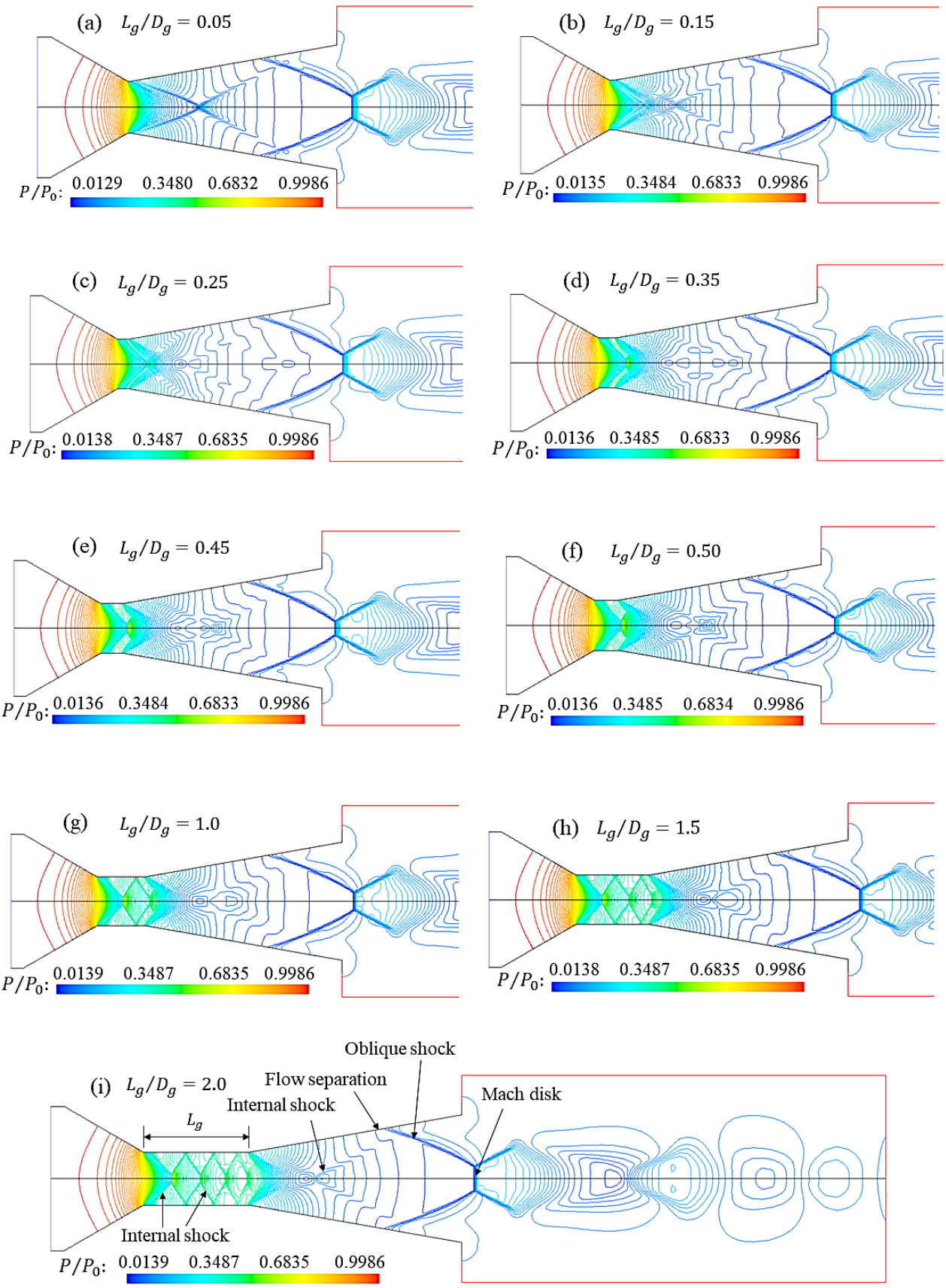

Figure 5. Flow field with presence of shock waves: pressure contour lines. Conical nozzle throat length in the range $0.05 \leq L_g/D_g \leq 2$. Source: Authors.

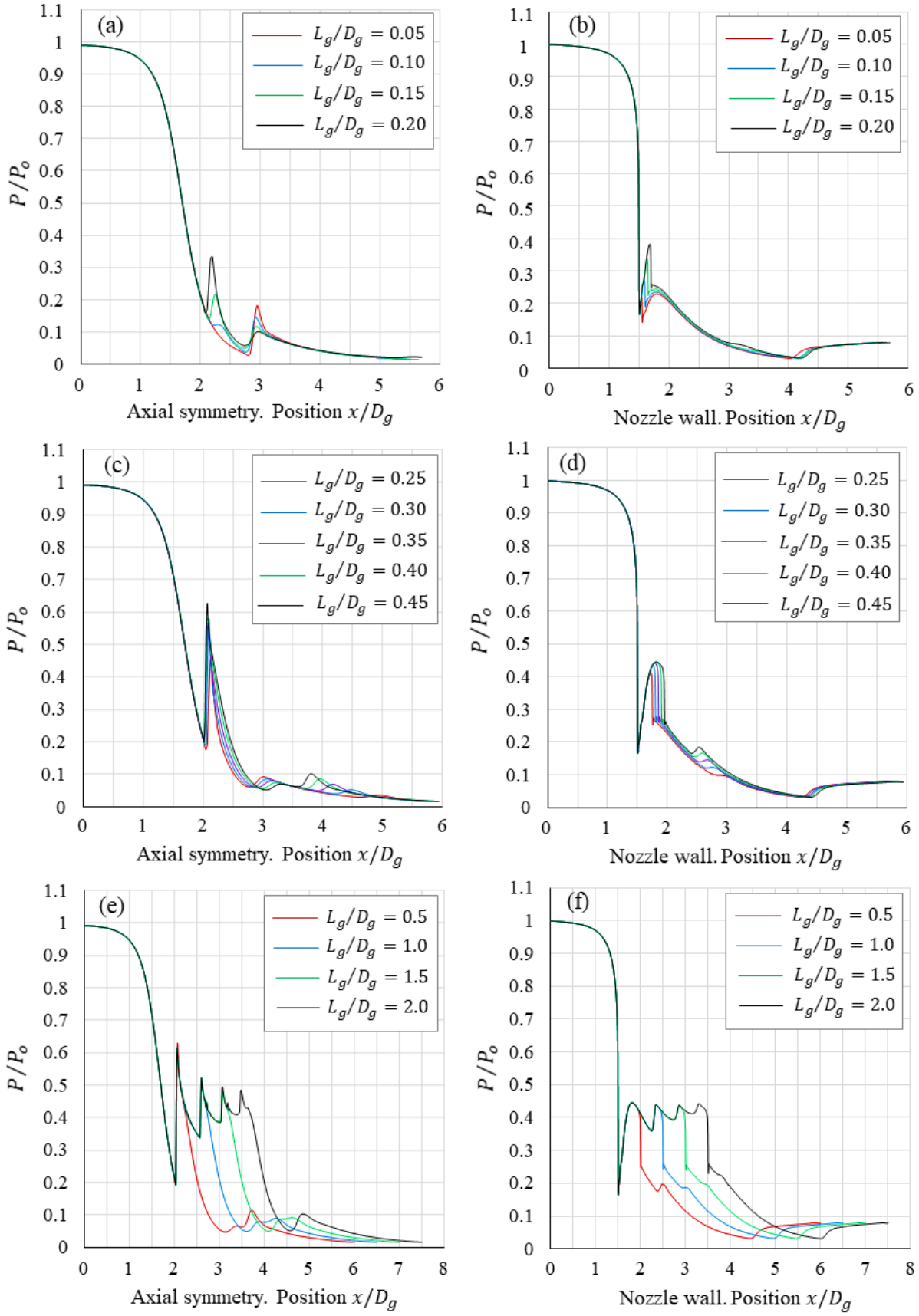

Figure 6.Pressure patterns. Throat length in the range (a) $0.05 \leq L_g/D_g \leq 0.2$; (b) $0.25 \leq L_g/D_g \leq 0.45$ y (c) $0.5 \leq L_g/D_g \leq 2$..Source: Authors.

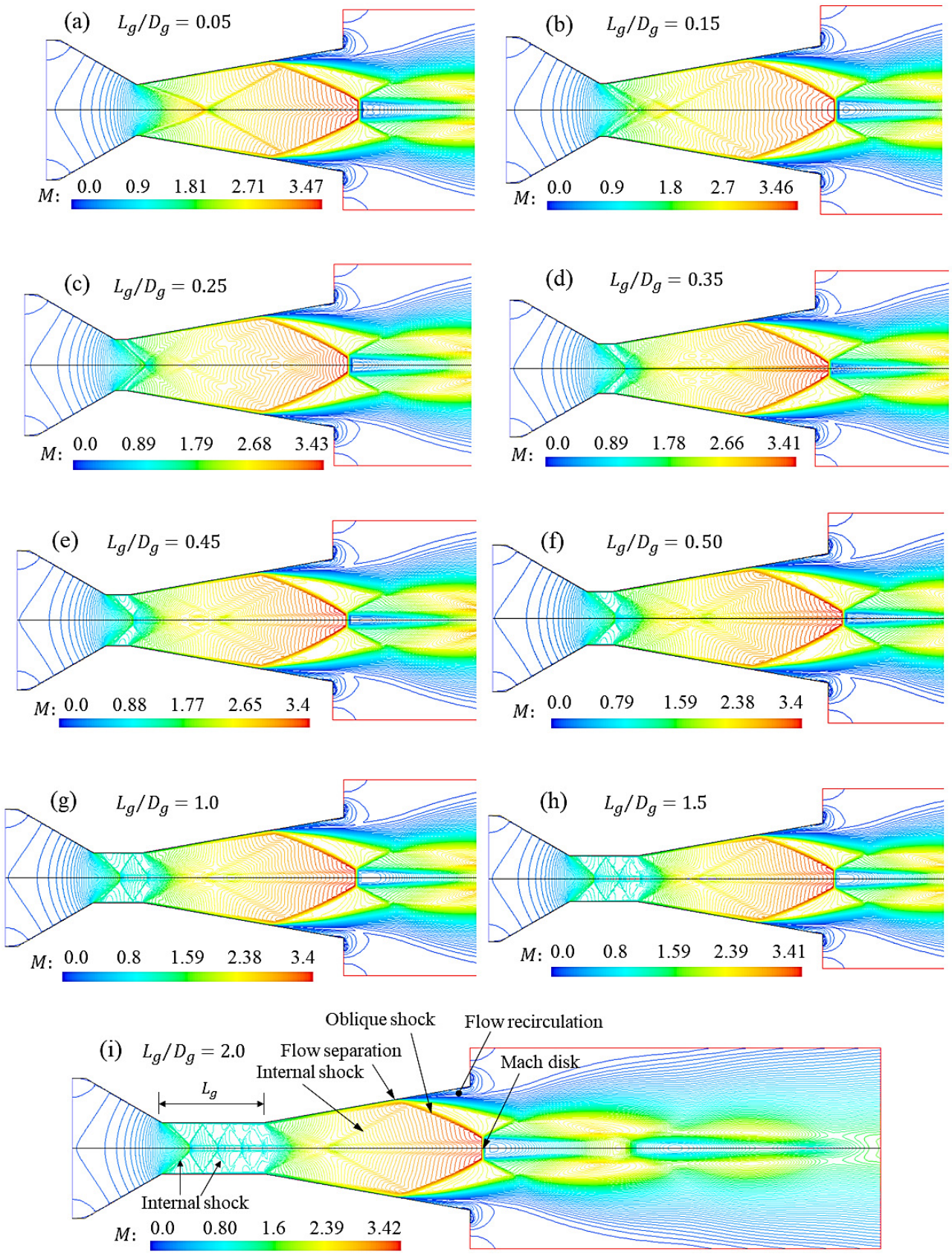

Figure 7. Flow field with presence of shock waves: Mach number contour lines. Conical nozzle throat length in the range $0.05 \leq L_g/D_g \leq 2$. Source: Authors.

The behavior of the Mach number patterns, for the range of positions from x/D_g = 1.5 to x/D_g = 3.5, for L_g/D_g = 0.5, L_g/D_g = 1, L_g/D_g = 1.5 and L_g/D_g = 2 show the minimum and maximum magnitudes reached by the flow velocity (Fig. 8c). The flow's accelerations and decelerations are not convenient since it increases pressure fluctuations and vibrations. And the increase in throat length contributes to the weight increase of the nozzle itself.

The wall of the throat section for L_g/D_g = 0.5 to L_g/D_g = 2 has no curvature. Therefore, the pressure loads on the throat section's wall surface are different from conventional nozzles, which have curvatures.

The pressure patterns in the throat section, axial symmetry, and wall are shown in Fig. 6. In the wall, pressure drops are observed at the throat inlet, and pressure increases in the throat section, with the pressure differences being of the lesser magnitude of the throat length range $0.05 \leq L_g/D_g \leq 0.2$, and of greater magnitude the pressure differences in the range of $0.25 \leq L_g/D_g \leq 2$.

On the divergent wall, the pressure patterns show drops, and after the separation of the flow due to the oblique shock, the pressure increases. The lateral pressure loads on the wall of the divergent for the internal flow are different from the pressure load of the ambient atmosphere, which is the external flow. Therefore, a pressure gradient is presented on the wall of the nozzle.

The internal flow region adjacent to the adiabatic wall of the divergent increases its temperature as a result of friction. In the central region, the flow has a much lower temperature as a result of the expansion. Where the start of flow separation occurs, there is a thermal shock due to temperature differences. The shock wave that occurs in the central region of the flow at the nozzle exit has a structure [14]. The extension of the analysis of the temperature and flow field through figures and graphs is beyond the scope of this work.

The transition of internal shock formation in the throat section as L_g increases in the range of $0.15 \leq L_g/D_g \leq 2$, shows that the length of the throat has a strong effect on the flow development. Therefore, a supersonic nozzle with a throat length that is too long is not suitable since it presents internal shocks, speed, and pressure fluctuations, which leads to increased vibrations and increased weight of the nozzle itself; however, for the range of $0.05 \leq L_g/D_g \leq 0.15$, the flow does not present internal shocks, in this sense, it is an adequate and optimal range of nozzles outside the design with throat length, for diameters around D_g = 20 mm Where, the length L_g corresponds to the range from 5 to 15% of the throat diameter D_g.

Similar results of internal shocks in conical nozzles with throat length were reported in [29-32], which were simulated with Menter's turbulence model [38]. The group of nozzles has values around L_g/D_g = 1. The normal and oblique shock occurs within the divergent, for the flow with NPR=7.23, and the velocity patterns are similar to those presented in Fig. 8c. Although the simulation of the nozzle with throat length reported in [31] has slight curvatures at the converging and diverging junctions and average divergent angles equal to and greater than 11°, they present the same Mach number pattern in the Axial symmetry in the throat section.

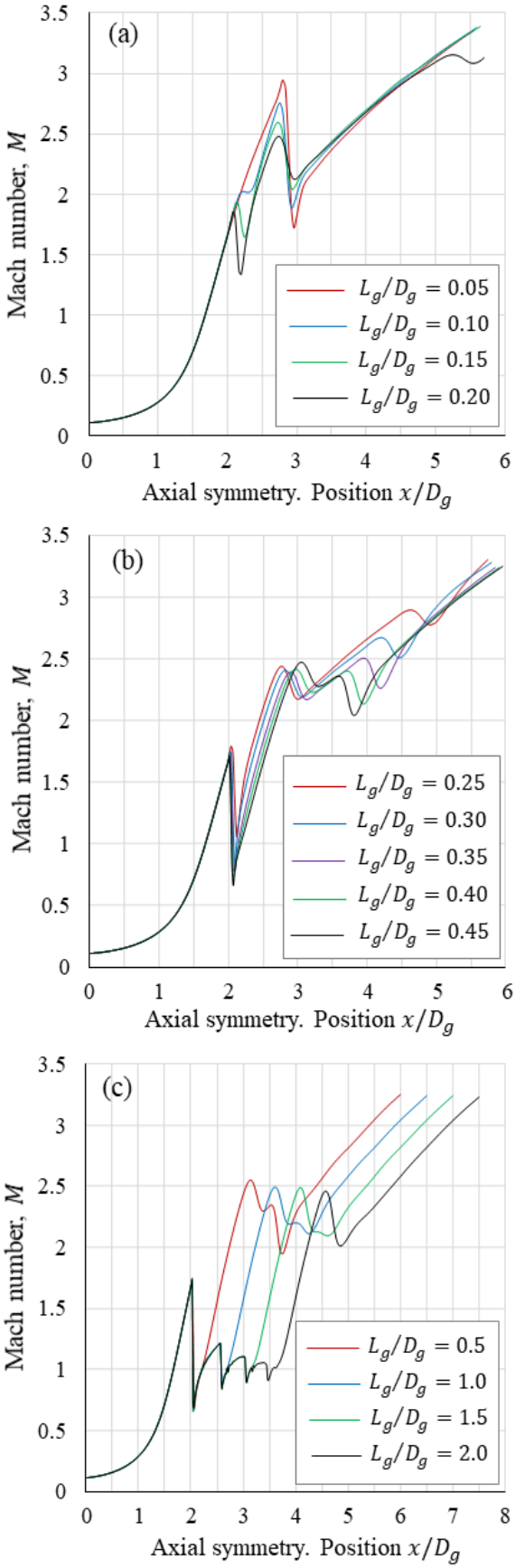

Figure 8. Mach number patterns. Throat length in the range (a) $0.05 \leq L_g/D_g \leq 2$; (b) $0.25 \leq L_g/D_g \leq 0.45$ (c) $0.5 \leq L_g/D_g \leq 2$. Source: Authors.

The results of the flow field and the Mach number and pressure patterns presented in Fig. 5, 6, 7, and 8 show the transition of the formation of the internal shocks in the throat section and the flow velocity reaching the nozzle outlet, which allows deepening the knowledge of the behavior of the flow in the throat section and in the divergent section as L_g increases.

It should be noted that these results could be taken into account as a reference to compare with other studies for viscous flow in low power nozzles, for the throat length range $0.05 \leq L_g/D_g \leq 0.15$, and for decreasing throat diameters up to $D_g = 1$ mm.

In the aspect of the manufacture of the nozzles, as their size decreases, the manufacture of the curvature of the throat becomes difficult, for example, for the throat diameter of 1 mm. In this sense, a throat length, L_g, is required to join the convergent and divergent sections.

4. CONCLUSIONS

The study of the flow field for a nozzle with $\alpha = 10°$, NPR=12 and different throat lengths, L_g in the range $0.05 \leq L_g/D_g \leq 2$ was determined, that there is a strong influence on the development of the flow in the throat section and in the divergent section as L_g increases.

In the throat section, for $L_g/D_g = 1$ the Mach num–ber was $0.6 < M$ M 1.8. For $L_g/D_g = 1$, the flow presented a staggering behavior of speed fluctuations, where the flow speeds up and slows down, with a damping tendency towards the end of the straight section of the throat to reach Mach 1 speed.

The flow did not present fluctuations in the throat section for the range of $0.05 \leq L_g/D_g \leq 0.15$. Therefore, the throat length in the range of 5 to 15% of the throat diameter is an optimal range, where the flow accelerates without disturbances and the presence of internal shocks.

REFERENCES

[1] Okninski, A., Marciniak, B., Bartkowiak, B., Kaniewski, D., Matyszewski, J., Kindracki, J. and Wolanski, P.: Development of the polish small sounding rocket program, Journal Acta Astronautica, Vol. 108, pp. 46–56, 2015, https://doi.org/10.1016/j.actaastro.2014.12.001

[2] Huh, J., Ahn, B., Kim, Y., Song, H., Yoon, H. and Kwon, S.: Development of a university-based simplified H_2O_2/PE hybrid sounding rocket at KAIST, International Journal of Aeronautical and Space Sciences, Vol. 18, No. 3, pp. 512–521, 2017, https://dx.doi.org/10.5139/IJASS.2017.18.3.512

[3] Villanueva, F.M.: Sounding rocket development program for Perú, in: *2018IEEE Aerospace Conference, Big Sky, MT*. pp. 1-9. https:// ieeexplore.ieee.org/abstract/document/8396555

[4] Nilsen, C., Meriam, S., Meyer, S.: Purdue liquid oxygen-liquid methane sounding rocket, in: *AIAA SciTech Forum, 2019, San Diego, California,* https://doi.org/10.2514/6.2019-0614

[5] Heeg, F., Kilzer, L., Seitz, R. and Stoll, E.: Design and test of a student hybrid rocket engine with an external carbon fiber composite structure, Aerospace,Vol. *7,* No. 57, pp. 1–19, 2020, https://doi.org/10.3390/aerospace7050057

[6] Marcano, V., Benítez, P., La Rosa, C., Lacruz, L., Parco, M.A., Ferreira, J., Andressen, R., Serra, A., Peñaloza, M., Rodríguez, L., Cárdenas, J.E., Minitti, V. and Rojas, J.J.: Progress reached in the universitary project cohetesonda ULA, Journal University, Science and Technology Vol.13, No. 53, pp. 305–316, 2009, (in Spanish), http://uct. unexpo.edu.ve/index.php/uct/article/view/109

[7] Tolentino, S.L., Nakka, R., Caraballo, S. and Mírez, J.:Numerical simulation of the flow under-expanded flow in the experimental conical nozzle helios-x, INGENIUS, No. 25, pp. 81–93, 2021, https://doi.org/10.17163/ings.n25.2021.08

[8] Sutton, G.P. and Biblarz, O.:*Rocket propulsion elements,* John Wiley and Sons, New York, 2016.

[9] Anderson, J.D.: *Fundamentalsof aerodynamics*, McGraw-Hill Education, New York, 2017.

[10] Martelli, E., Saccoccio, L., Ciottoli, P., Tinney, C., Baars, W. and Bernardini, M.: Flow dynamics and wall-pressure signatures in a high-Reynolds-number overexpanded nozzle with free shock separation, Journal of Fluid Mechanics, Vol. 895, pp. A29 1-30, 2020, doi:10.1017/jfm.2020.280

[11] Mahapatra, S., Nelaturi, A., Tennyson, J.A. and Ghosh, S.: Large-eddy simulation of compressible turbulent flow in convergent-divergent nozzles with isothermal wall, International Journal of Heat and Fluid Flow, Vol. 78, pp. 1-20, 2019, https: //doi.org/10.1016/j.ijheatfluidflow.2019.108425

[12] Schlichting, H. and Gersten, K.: *Boundary-layer theory*, Springer-Verlag, Berlin Heidelberg, Germany, 2017.

[13] Karman, T.V.: The fundamentals of the statistical theory of turbulence, Journal of the Aeronautical Sciences, Vol. 4, No. 4, pp. 131–138, 1937, https://doi.org/10.2514/8.350

[14] Génin, C., Stark, R. and Karl, S.: Shock system deformation in high Mach number rocket nozzles, in *Sasoh A., Aotki T., Katayama M. (eds) 31st International Symposium on Shock Waves 2, ISSW 2017*. Springer, Cham., 2019, pp. 543-549, https://doi.org/10.1007/978-3-319-91017-8_69

[15] Génin, C., Stark, R.: Hot Flow Testing of Dual Bell Nozzles. In *49th AIAA Aerospace Sciences Meeting Including the New Horizons Forum and Aerospace Exposition.* 2011, pp. 1-8.

[16] Riveros, F.A. and Rodriguez, L.A.: *Design and construction of a hobbyist rocket controlled by actuation of a vector thrust nozzle (in Spanish)*, Degree work, Faculty of Eng, Nueva Granada Military University, Bogotá, Colombia, 2010.

[17] Krehl, P. and Engemann, S.: August Toepler - the first who visualized shock waves, Shock Waves, Vol. 5, No. 1, pp. 1–18, 1995, https://doi.org/10.1007/BF02425031

[18] Blazek, J.: *Computational fluid dynamics: principles and applications*, Oxford, United Kingdom: Butterworth-Heinemann, 2015.

[19] Wilcox, D.C.: *Turbulence modeling for CFD*. C., California, USA: DCW Industries, 2006.

[20] Kostić, O.P., Stefanović, Z.A., Kostić, I.A.: CFD modeling of supersonic airflow generated by 2D nozzle with and without an obstacle at the exit section, FME Transactions, Vol. 43, No. 2, pp. 107-113, 2015.

[21] Zmijanović, V., Rašuo, B., Chpoun, A.: Flow separation modes and side phenomena in an overexpanded nozzle, FME Transactions, Vol. 40, No. 3, pp. 111-118, 2012.

[22] Živković, S., M Milinović, M., Adamec, N.: Experimental and numerical research of a supersonic planar thrust vectoring nozzle via mechanical tabs, FME Transactions Vol. 42 No. 3, pp. 205-211, 2014.

[23] Cuffel, R.F. Back, L.H. and Massier, P.F.: Transonic flow field in a supersonic nozzle with small throat radius of curvature. AIAA Journal, Vol.7, No. 7, pp. 1364–1366, 1969. https://doi.org/10.2514/3.5349

[24] Sauer, A.: General characteristics of the flow through nozzles at near critical speeds, NACA TM-1147, 1947.

[25] Back, and R.F. Cuffel, R.F.: Flow coefficients for supersonic nozzles with comparatively small radius of curvature throats, AAIA Journal, Vol. 8, No. 2, pp.196-198, 1970.

[26] Kliegel, R. and Levine, J.N.: Transonic flow in small throat radius of curvature nozzles, AAIA journal, Vol. 7, No. 7, pp. 1375-1378, 1969.

[27] Haddad, A. andKbab, H.: Application of De-Laval nozzle transonic flow field computation approaches, International Journal of Mechanical, Aerospace, Industrial, Mechatronic and Manufacturing Engineering, Vol:7, No. 2, pp. 318-323, 2013.

[28] Ordoñez, G.: *Design, manufacture and experimentation of a jet engine for research purposes (in Spanish)*, Master's degree work, Faculty of Mechanical Engineering, National University of Engineering (UNI), Lima, Perú, 2014.

[29] Tolentino, S.L., Ferreira, J., Parco, M.A., Lacruz, L. and Marcano, V.: Numerical simulation of the flow over-expanded in the experimental conical nozzle ULA-1A XP, Journal University, Science and Technology, Vol. 21, No. 84, pp. 126–133, 2017, (in Spanish), http://www.uct.unexpo.edu.ve/index .php/uct/article/view/803

[30] Tolentino, S.L. and Mírez, J.: Numerical analysis of over-expanded flow in the experimental ULA-2 conical nozzle out of design, Lámpsakos, No 24, pp. 33-47, 2020, (in Spanish), https://doi.org/10.21501/214540863707

[31] Tolentino, S.L., Parco, M.A., Caraballo, S., Lacruz, L., Marcano, V., Ferreira, J. and Mírez, J.: Numerical analysis of the flow behavior in the throat section of an experimental conical nozzle, Journal Enfoque UTE, Vol. 12, No. 1, pp. 12–28, 2021, (in Spanish), https://doi.org/10.2909/enfoqueute.676

[32] Tolentino, S.L. and González, O.: Numerical analysis of the over-expanded flow in the experimental conical nozzle ULA-1B out of design, Lámpsakos, No 24, pp. 33-47, 2021, (in Spanish), https://doi.org/10.21501/214540863707

[33] ANSYS, Ansys Fluent 12.0 Theory guide, https://www.afs.enea.it/project/neptunius/docs/fluent/html/th/main_pre.htm

[34] F. White, *Fluids Mechanics*, McGraw-Hill Education, New York, 2016.

[35] Spalart, P.R. and Allmaras, S.R.: A one-equation turbulence model for aerodynamic flows", *30th Aerospace Sciences Meeting and Exhibit, 06 January 1992 – 09*, Reno, NV, U.S.A, 1992, pp. 1-22, https://doi.org/10.2514/6.1992-439

[36] Sutherland, W.: The viscosity of gases and molecular force, Philosophical Magazine series 5, Vol. 36, No. 223, pp. 507–531, 1893,

[37] Hunter, C.A.: Experimental, theoretical, and computational investigation of separated nozzle flows, *34thAIAA/ASME/SAE/ASEE Joint Propulsion Conference* & exhibit, Cleveland, OH, July 1998, https://doi.org/10.2514/6.1998-3107

[38] Menter, F.: Two equation eddy-viscosity Turbulence models for engineering applications. AIAA Journal, Vol. 32, pp. 1598-1605, 1994.

[39] Tolentino, S.L.: Evaluation of turbulence models for the air flow in a planar nozzle, INGENIUS, No. 22, pp. 25–37, 2019.

ЕФЕКАТ ДУЖИНЕ ГРЛА НА ОБРАСЦЕ ПРОТОКА У КОНУСНИМ МЛАЗНИЦАМА ВАН ДИЗАЈНА

С.Л. Толентино, Х. Мирес

У овом раду је спроведена теренска студија струјања за конусне млазнице ван дизајна са некружним цилиндричним деловима грла, као што су они који се налазе у експерименталним апли–кацијама сондажних ракетних мотора. Поље протока је симулирано РАНС моделом у АНСИС-Флуент Р16.2 коду за 2Д домене. Коришћене главне једначине су очување масе, импулса, енергије и стања. Сатерлендова једначина за вискозност као функцију температуре и Спаларт-Аллмарасов мо–дел турбуленције коришћени су за симулацију турбуленције прекомерно проширеног струјања. Резултати су показали флуктуације притиска и Маховог броја како се дужина грла повећавала. У делу грла се закључује да се за опсег дужине од 5 до 15% пречника грла ток убрзава без присуства унутрашњег шока.